ISSN 1674-1056
http://cpb.iphy.ac.cn
http://iopscience.iop.org/cpb
中国物理 B
Chinese Physics
中国物理 Chinese Physics B

Structural, electronic, vibrational, and thermodynamic properties of $Zr_{1-x}Hf_xCo$: A first-principles-based study

Jun-Chao Liu(刘俊超), Zhi-Hong Yuan(袁志红), Shi-Chang Li(李世长), Xiang-Gang Kong(孔祥刚), You Yu(虞游), Sheng-Gui Ma(马生贵), Ge Sang(桑革), Tao Gao(高涛)
Citation: Chin. Phys. B . 2018, 27(4): 047802. **doi:** 10.1088/1674-1056/27/4/047802

Journal homepage: http://cpb.iphy.ac.cn; http://iopscience.iop.org/cpb

What follows is a list of articles you may be interested in

Optimization of a poly(*p*-phenylene benzobisoxazole)-based light-emitting device with a complex cathode structure

Zhang Xiao-Jin, He Zhi-Qun, Wang Jing, Mu Lin-Ping, Zhao Huan, Liang Chun-Jun, Zhuang Qi-Xin, Han Zhe-Wen
Chin. Phys. B . 2013, 22(11): 117805. **doi:** 10.1088/1674-1056/22/11/117805

Density functional theory study of NO_2-sensing mechanisms of pure and Ti-doped WO_3 (002) surfaces

Hu Ming, Wang Wei-Dan, Zeng Jing, Qin Yu-Xiang
Chin. Phys. B . 2011, 20(10): 102101. **doi:** 10.1088/1674-1056/20/10/102101

Ab-initio density functional theory study of a WO_3 NH_3-sensing mechanism

Hu Ming, Zhang Jie, Wang Wei-Dan, Qin Yu-Xiang
Chin. Phys. B . 2011, 20(8): 082101. **doi:** 10.1088/1674-1056/20/8/082101

Structural, electronic, vibrational, and thermodynamic properties of $Zr_{1-x}Hf_xCo$: A first-principles-based study*

Jun-Chao Liu(刘俊超)[1,2], Zhi-Hong Yuan(袁志红)[1], Shi-Chang Li(李世长)[1], Xiang-Gang Kong(孔祥刚)[1], You Yu(虞游)[3], Sheng-Gui Ma(马生贵)[1], Ge Sang(桑革)[4], and Tao Gao(高涛)[1,†]

[1] *Institute of Atomic and Molecular Physics, Sichuan University, Chengdu* 610065, *China*
[2] *College of Physical Science and Technology, Sichuan University, Chengdu* 610065, *China*
[3] *College of Optoelectronic Technology, Chengdu University of Information Technology, Chengdu* 610225, *China*
[4] *Science and Technology on Surface Physics and Chemistry Laboratory, P. O. Box* 9071-35, *Jiangyou* 621907, *China*

(Received 27 November 2017; revised manuscript received 15 January 2018; published online 10 March 2018)

The physical properties including structural, electronic, vibrational and thermodynamic properties of $Zr_{1-x}Hf_xCo$ (x is the concentration of constituent element Hf, and changes from 0 to 1) are investigated in terms of the ABINIT program. The results reveal that all of $Zr_{1-x}Hf_xCo$ have similar physical properties. When Hf concentration x gradually increases from 0.0 to 1.0, the lattice constant decreases from 3.217 Å to 3.195 Å very slowly. The calculated density of states (DOS) indicates that the metallic nature is enhanced and the electrical conductivity turns better with the increase of Hf. Moreover, as Hf concentration increases from 0 to 1, the Fermi energy gradually increases from −6.96 eV to −6.21 eV, and the electronic density of states at the Fermi level ($N(E_f)$) decreases from 2.795 electrons/eV f.u. down to 2.594 electrons/eV f.u., both of which imply the decrease of chemical stability. The calculated vibrational properties show that the increase of Hf concentration from 0 to 1 causes the maximum vibrational frequency to decrease gradually from about 223 cm^{-1} to 186 cm^{-1}, which suggests a lower dispersion gradient and lower phonon group velocities for these modes. Finally, the phonon related thermodynamic properties are obtained and discussed.

Keywords: $Zr_{1-x}Hf_xCo$, electronic properties, vibrational properties, thermodynamic properties

PACS: 78.30.Er, 21.65.–f, 21.60.De **DOI:** 10.1088/1674-1056/27/4/047802

1. Introduction

The intermetallic compound ZrCo has received considerable attention because it is a probable candidate material for the storage and delivery of hydrogen isotopes in the international thermonuclear experimental reactor team (ITER). Compared with uranium conventionally serving as a getter in ITER, ZrCo has some inherent advantages, e.g., no radioactivity, less pyrophoricity, easier to operate. Moreover, ZrCo has excellent hydriding/dehydriding properties, such as the extremely low equilibrium absorption pressure (down to 10^{-2} Pa at room temperature for tritium recovery), and the not too high dehydrogenation temperature (approximately 400 °C when dissociation hydrogen pressure reaches 1 atm, 1 atm = 1.01325×10^5 Pa).[1–7] Therefore, ZrCo has been selected and used to store and transport hydrogen isotopes by ITER.[8,9]

Many experimental researches on the $Zr_{1-x}M_xCo$ system in which Zr atom is partially substituted for by other kind of atom M, such as Ti and Hf, confirm that some kind of element substitution can inhibit the disproportionation reaction, which is easily induced in the course of the hydrogen recovery/delivery processes of ZrCo thereby making ZrCo lose its ability to store hydrogen isotopes.[5,10–15]

However, to the best of our knowledge, no theoretical ab-initio study on the $Zr_{1-x}M_xCo$ system has been reported except the ZrCo and HfCo. Li *et al.*[16] investigated the vibrational and thermodynamic properties of ZrCo by density functional perturbation theory (DFPT). Chattaraj *et al.*[17,18] reported the structural, electronic, vibrational, thermodynamic and elastic properties of ZrCo by using a first principles approach within the Vienna *ab initio* simulation package (VASP). In addition, Chattaraj *et al.*[19] measured the enthalpy increments of $Zr_{0.5}Co_{0.5}$ in a temperature range of 642 K–1497 K, then the thermodynamic functions of $Zr_{0.5}Co_{0.5}$ in a temperature range of 298.15 K–1500 K were obtained through the measuring enthalpy increments. Recently, Lu *et al.*[20] investigated structural, elastic, and electronic properties of CoZr under high pressure by first-principles study, and confirmed that CoZr is mechanically stable at various pressures and the structural stability decreases under high pressure.

Here, we aim at studying the structural, electronic, dynamic, and thermodynamic properties of $Zr_{1-x}Hf_xCo$ (x is the concentration of constituent element Hf, and changes from 0 to 1 in steps of $\Delta x = 0.1$, the x has the same meaning in this paper, unless otherwise stated) by first-principles study.

*Project supported by the National Natural Science Foundation of China (Grant No. 21573200).
†Corresponding author. E-mail: gaotao@scu.edu.cn
© 2018 Chinese Physical Society and IOP Publishing Ltd

The rest of this paper is arranged as follows. In Section 2, we give a detailed description of the computational method. In Section 3, the acquired results and their interpretation are given. Finally, a brief summary is given in Section 4.

2. Computational details

All the calculations in this work are performed through the density functional theory (DFT) and DFPT in the plane-wave pseudopotential approach by using the ABINIT code.[21] The generalized gradient approximation (GGA) of Perdew–Burke–Ernzerhof (PBE)[22] is adopted for exchange–correlation energy, and the electronic pseudo-potentials are used for atoms Zr-$4s^2 4p^6 4d^2 5s^2$, Co-$3s^2 3p^6 3d^7 4s^2$, and Hf-$5s^2 5p^6 5d^2 6s^2$, respectively. According to our convergence test, an $8\times8\times8$ Monkhorst-pack k-point mesh in the Brillouin zone for one unit cell is used, and the energy cut-off is set with 30 Hartree (1 Hartree = 4.3597×10^{-18} J) to determine the number of plane waves in expansion which guarantees the total energy errors within 10^{-10} Hartree in all our calculations. After structural optimization, the detailed vibrational properties including the phonon dispersion curves, phonon density of states, and phonon frequencies at zone-center are obtained by the DFPT. Thereafter, thermodynamic properties such as internal energy E, entropy S, and specific heat C_V are predicted within the harmonic approximation, then Gibbs free energy G is computed through the obtained internal energy E and entropy S.

The virtual crystal approximation (VCA)[23] implemented in the ABINIT program is used to simulate the disordered alloy $Zr_{1-x}Hf_xCo$. Two main approaches exist for treating the disordered alloy within first principles methods: the supercell (SC) method and the VCA method. The SC method can give more correct results but the calculation time becomes rapidly too large compared with the VCA method.[24] In contrast to this, the VCA method has the advantages of simplicity and computational efficiency because the VCA allows the crystal to remain the primitive periodicity but contains some fictitious "virtual" atoms whose potential is the average of potentials of the atoms in the parent compounds.[24–26] So, the VCA method is an alternative and a promising approach to treating the disordered alloys and has successfully predicted the physical properties, including structural, electronic, piezoelectric, elastic, magnetic, metal, and dynamic properties of many disordered alloy systems.[24,25,27–32]

Therefore, we believe that the VCA method is a reliable method of predicting the electronic, vibrational, and thermodynamic properties of the ternary $Zr_{1-x}Hf_xCo$ alloy. In the $Zr_{1-x}Hf_xCo$ system, the virtual pseudo-potential of a virtual atom is obtained by the linear combination of elemental ionic pseudo-potentials of ZrCo and HfCo within first-principles VCA scheme, that is to say, $V_{VCA} = (1-x)V_{ZrCo} + xV_{HfCo}$, where x is the Hf substitute fraction.

3. Results and discussion

3.1. Structural properties

Experiments[15,33,34] have confirmed that solid solution $Zr_{1-x}Hf_xCo$ ($x = 0.1$, 0.2, 0.25, 0.3, 0.5, 0.75) are rather stable and that crystal structures of $Zr_{1-x}Hf_xCo$ are identical with those of alloys ZrCo and HfCo. That is to say, $Zr_{1-x}Hf_xCo$ ($x = 0.1$, 0.2, 0.25, 0.3, 0.5, 0.75) are of CsCl type simple cubic structure with space group of $Pm\bar{3}m$ (No. 221).[35] Therefore, we believe that all of $Zr_{1-x}Hf_xCo$ ($x = 0.1 \sim 0.9$) have the same crystal structures as ZrCo and HfCo. In the subsequent calculation, we work starting from the above structure properties.

Table 1. Optimized and experimental lattice constants of $Zr_{1-x}Hf_xCo$, x represents the concentration of constituent element Hf.

x	0.0	0.1	0.2	0.3	0.4	0.5	0.6	0.7	0.8	0.9	1.0
This wok	3.227	3.225	3.224	3.222	3.219	3.216	3.212	3.208	3.204	3.200	3.195
Other cal.	3.203[a] 3.181[b]										
Expt.	3.201[c] 3.196[d]					3.173[d]					3.166[d]

[a]Ref. [16], [b]Ref. [17], [c]Ref. [36], [d]Ref. [34]

The equilibrium lattice parameter is computed from the structural optimization, using the Broyden–Fletcher–Goldfarb–Shanno minimization.[37–40] The results of optimization for $Zr_{1-x}Hf_xCo$ along with other theoretical and experimental results are listed in Table 1. It can be seen that our calculated lattice constants for $Zr_{1-x}Hf_xCo$ are very close to other theoretical[16,17] and experimental results,[34,36] which ensures the accuracy and the reliability of our further study of $Zr_{1-x}Hf_xCo$.

From Table 1, we can see that the lattice constant gradually decreases from 3.227 Å to 3.195 Å with the increase of the Hf substitute rate, but change is quite small. A slight change of lattice constant is logical for the reason that atom Hf and atom Zr have similar valence electronic configurations and almost the same atom radius. The decrease of lattice constant means that the crystal plane spacing of ZrCo is bigger than

that of HfCo, which is in agreement with experimental results reported by Peng *et al.*[15]

3.2. Electronic properties

In order to understand the effect of Hf-doping on the electronic behavior of $Zr_{1-x}Hf_xCo$, we calculate the density of states (DOS) of $Zr_{1-x}Hf_xCo$ around the Fermi level, some of them are shown in Fig. 1. The calculated results reveal that $Zr_{1-x}Hf_xCo$ have similar DOSs for different Hf substitute ratios, which implies that all of $Zr_{1-x}Hf_xCo$ exhibit similar electronic properties. The reason for this phenomenon is that element Hf and element Zr belong to the same family, atom Hf and atom Zr have similar valence electronic configurations. Further analysis shows that above the Fermi level, with the increase of Hf concentration from 0 to 1, the energy range expands and the peak value (around 4 eV) of DOS decreases from 6.085 electrons/eV f.u. to 4.235 electrons/eV f.u. That is to say, the DOS shifts towards the high energy and the Fermi surface moves down with Hf content increasing. All these phenomena show that the nature of metal is strengthened with increasing Hf content. Consequently, it can be predicted that as the Hf concentration gradually increases, the conductivity is getting better.[20,32]

Fermi energy and the electron density of states at the Fermi level $N(E_f)$ can describe the stability of the compound and the strength of electron interaction. The Fermi energy and the electronic density of states at the Fermi level $N(E_f)$ are given in Fig. 2. Figure 2(a) shows that the higher the concentration of Hf, the higher the Fermi energy is, which induces the lower chemical stability of the compound and lattice contraction. Moreover, one can see from Fig. 2(b) that the $N(E_f)$ decreases with the increase of Hf content, which implies that orbital hybridization between $Zr_{1-x}Hf_x$ and Co in the region near the Fermi level and the electronic interaction of the atomic orbital weaken. This phenomenon also indicates that the chemical stability decreases as the Hf content increases.[17,20]

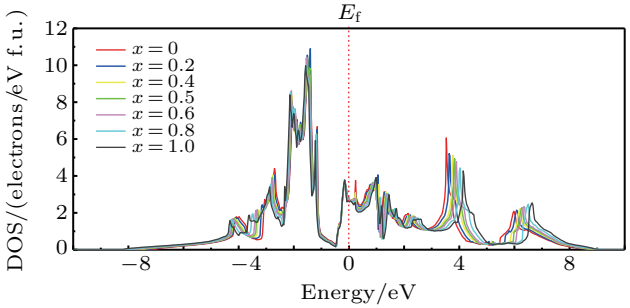


Fig. 1. (color online) Plots of DOS versus energy for $Zr_{1-x}Hf_xCo$ with $x = 0.0$, 0.2, 0.4, 0.5, 0.6, 0.8, and 1.0.

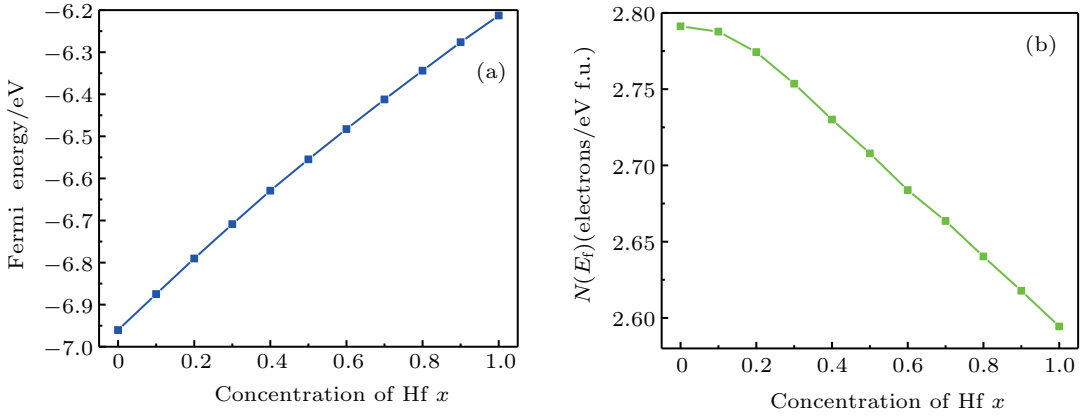


Fig. 2. (color online) (a) Hf concentration dependence of Fermi energy. (b) Hf concentration dependence of TDOS at Fermi level $N(E_f)$.

3.3. Vibrational properties

Herein, the detailed vibrational properties of $Zr_{1-x}Hf_xCo$ are obtained by the DFPT. The calculated phonon dispersion curves (along the principal symmetry direction of the Brillouin zone $X \to M \to \Gamma \to R \to X \to \Gamma \to M$) and the corresponding total phonon density of states for $Zr_{1-x}Hf_xCo$ ($x = 0.0$, 0.5, 1.0) are plotted in Fig. 3. Evidently, an increase in the Hf content leads to the phonon frequency decreasing. Since the primitive cell of $Zr_{1-x}Hf_xCo$ contains two atoms, the corresponding numbers of vibrational modes are six, of which three are acoustic modes and the remaining modes are optical ones. According to the standard group-theoretical analysis, we can obtain the following irreducible representation at the Γ point:

$$\Gamma_{\text{acoustic}} = 3T_{1u}(\text{IR}); \quad \Gamma_{\text{optical}} = 3T_{1u}(\text{IR}),$$

where the IR represents infrared active modes, subscript u denotes the antisymmetric mode with respect to the center of inversion, and T_{1u} is the three-fold degenerate mode. The calculated phonon frequencies at the Γ point are listed in Table 2. As the Hf concentration gradually increases from 0.0 to 1.0, the calculated phonon frequencies of the optical modes at the Γ point gradually decrease from 184.28 cm^{-1} to 173.18 cm^{-1}, which is due to the mass effect. Unfortunately, we are not aware of any experimental reports on the vibrational properties of $Zr_{1-x}Hf_xCo$, but our results of ZrCo are in agreement with the other theoretical results.[18]

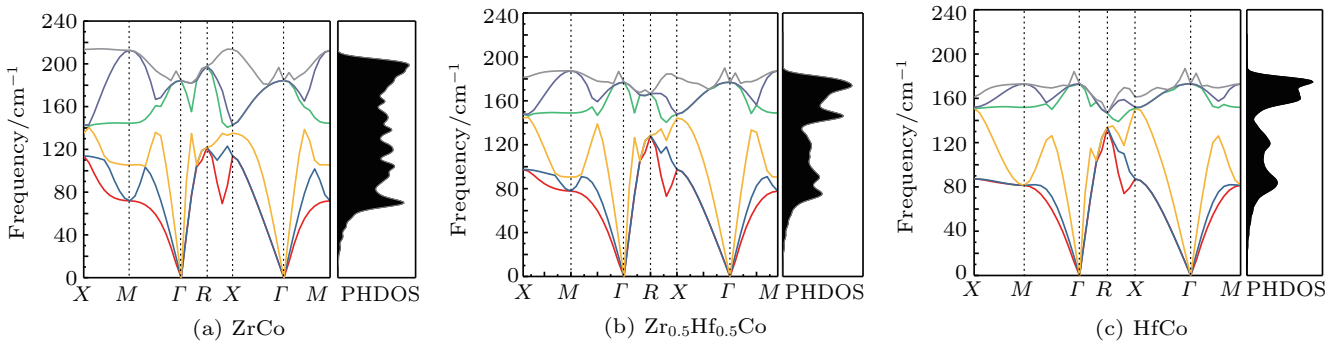


Fig. 3. (color online) Calculated phonon dispersion curves and the phonon densities of states for (a) ZrCo, (b) $Zr_{0.5}Hf_{0.5}Co$, and (c) HfCo.

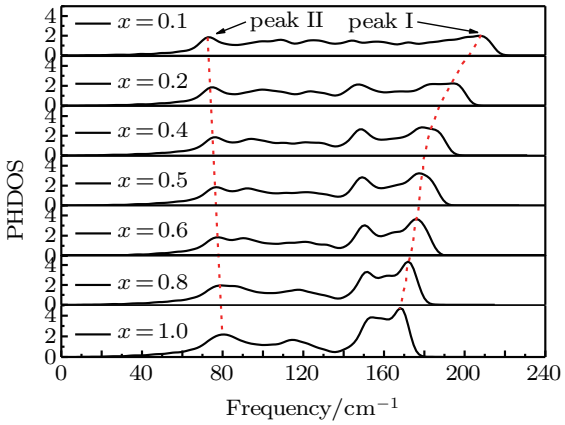


Fig. 4. (color online) Plots of PHDOS versus frequency of $Zr_{1-x}Hf_xCo$.

Figure 4 gives the calculated phonon density of states (PHDOS) for $Zr_{1-x}Hf_xCo$ ($x = 0.0$, 0.2, 0.4, 0.5, 0.6, 0.8, and 1.0). Two main peaks appear in Fig. 4, peak I significantly moves towards a low wave number with the increase of Hf concentration. Additionally, the increase of Hf concentration from 0 to 1 leads to the highest frequency mode gradually decreasing from about 223 cm^{-1} down to about 186 cm^{-1}, which implies a lower dispersion gradient and then lower phonon group velocities for these modes.[41] The reason for this phenomenon is that the atomic weight of the Hf atom is 1.96 times larger than that of the Zr atom, which leads to the increase of the reduced mass, therefore the vibrational frequency will decrease with the content of Hf increasing.

On the contrary, peak II of the phonon density of states slightly shifts towards a high wave number, which is due to the fact that vibrational frequency relates to the reduced mass of $Zr_{1-x}Hf_xCo$ and interaction between $Zr_{1-x}Hf_x$ and Co. Specifically, the stronger interaction between $Zr_{1-x}Hf_x$ and Co will result in the higher vibrational frequency of $Zr_{1-x}Hf_xCo$ and the larger reduced mass will bring about the lower vibrational frequency. For $Zr_{1-x}Hf_xCo$, the influence of interaction between $Zr_{1-x}Hf_x$ and Co on vibrational frequency may be more important than the reduced mass.

Table 2. Calculated optical mode T_{1u} at the Γ point of $Zr_{1-x}Hf_xCo$, (x represents the concentration of constituent element Hf).

x	0.0	0.1	0.2	0.3	0.4	0.5	0.6	0.7	0.8	0.9	1.0
This wok	184.28	182.09	180.38	178.92	177.89	177.01	176.48	175.64	174.73	173.87	173.18
Other cal.[a]	177.27										

[a] Ref. [18]

3.4. Thermodynamic properties

Knowledge of the thermodynamic properties is essential for studying crystal stability and chemical reactivity, but there are no publications focusing on thermodynamic properties of $Zr_{1-x}Hf_xCo$ except the ZrCo. As is well known, the first-principles for phonon calculations are limited to $T = 0$ K yet the detailed thermodynamic properties including internal energy E, entropy S, constant-volume specific heat C_V per unit cell of the crystals could be derived by phonons.[42]

In order to ensure the accuracies of thermodynamic properties for $Zr_{1-x}Hf_xCo$ with the VCA method, here we perform an ordered SC calculation of $Zr_{0.5}Hf_{0.5}Co$. The thermodynamic properties for $Zr_{0.5}Hf_{0.5}Co$ are obtained by the VCA and the SC methods and listed in Table 3. The ZrCo supercell is built with the $2 \times 1 \times 2$ of a unit cell, there are two of Zr positions substituted for by elements Hf as shown in Fig. 5. The supercell contains two Zr, two Hf and four Co atoms, and its constituent can be reduced to the formula $Zr_{0.5}Hf_{0.5}Co$. As can be seen from Table 3, the calculated thermodynamic results obtained with the two methods are almost equal and the maximum error is less than 0.3%. Hence, we believe that the VCA method is a reliable method for predicting the thermodynamic properties of the ternary $Zr_{1-x}Hf_xCo$ alloy.

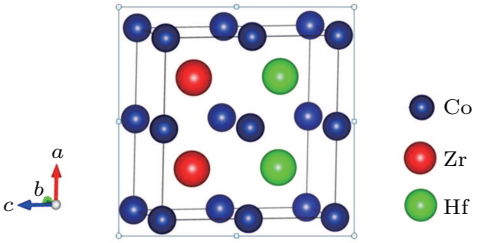


Fig. 5. (color online) Crystal structure of $Zr_{0.5}Hf_{0.5}Co$.

Table 3. Calculated results of the internal energy E (K·J/mol), entropy S (J/mol·K), and constant-volume specific heat C_V (J/mol·K) per unit cell for $Zr_{1-x}Hf_xCo$ at different values of temperature T (K), obtained with the VCA method and SC method.

T	E/(K·J/mol)		S/(J/mol·K)		C_V/(J/mol·K)	
	VCA	SC	VCA	SC	VCA	SC
0	4.751	4.755	0	0	0	0
100	6.502	6.508	27.521	27.552	36.869	36.912
200	10.778	10.780	56.799	56.801	46.044	46.066
300	15.517	15.521	75.941	75.988	48.121	48.130
400	20.370	20.372	89.903	89.952	48.882	48.891
500	25.276	25.278	100.854	100.912	49.240	49.243
600	30.209	30.11	109.850	109.921	49.436	49.438
700	35.159	35.160	117.481	117.523	49.555	49.557
800	40.118	40.120	124.103	124.156	49.633	49.634
900	45.083	45.084	129.952	129.968	49.686	49.688
1000	50.054	50.051	135.189	135.213	49.724	49.726

Gibbs free energy G is another important thermodynamic quantity. In the hydriding/dehydriding reaction the change of G can be used to determine the direction of the reaction. As is well known, the G can be obtained from the following formula:

$$G = H - TS,$$

where T and S are the temperature and entropy, respectively. H is the enthalpy, which can be expressed as

$$H = E + PV,$$

so

$$G = E - TS + PV$$

for solid and liquid phase, the value of PV at atmospheric pressure is very small compared with that of Gibbs free energy G, so PV can be ignored. Then, the G can be expressed as

$$G = E - TS.$$

The calculated values of E, S, C_V, and G at temperatures from 0 K to 1000 K are illustrated in Figs. 6(a)–6(d), respectively (the corresponding data for E, S, C_V, and G are provided in the supplementary materials from Table S1 to Table S4).

From Fig. 6, one can see that the differences among these thermodynamic quantities for $Zr_{1-x}Hf_xCo$ are very small, whereas the further analysis reveals that the increase of Hf content can cause the thermodynamic quantities to have some changes. In detail, as the Hf content increases, the calculated value of the internal energy E and Gibbs free energy G decrease, while the entropy S and constant-volume specific heat C_V increase in the selected temperature ranges.

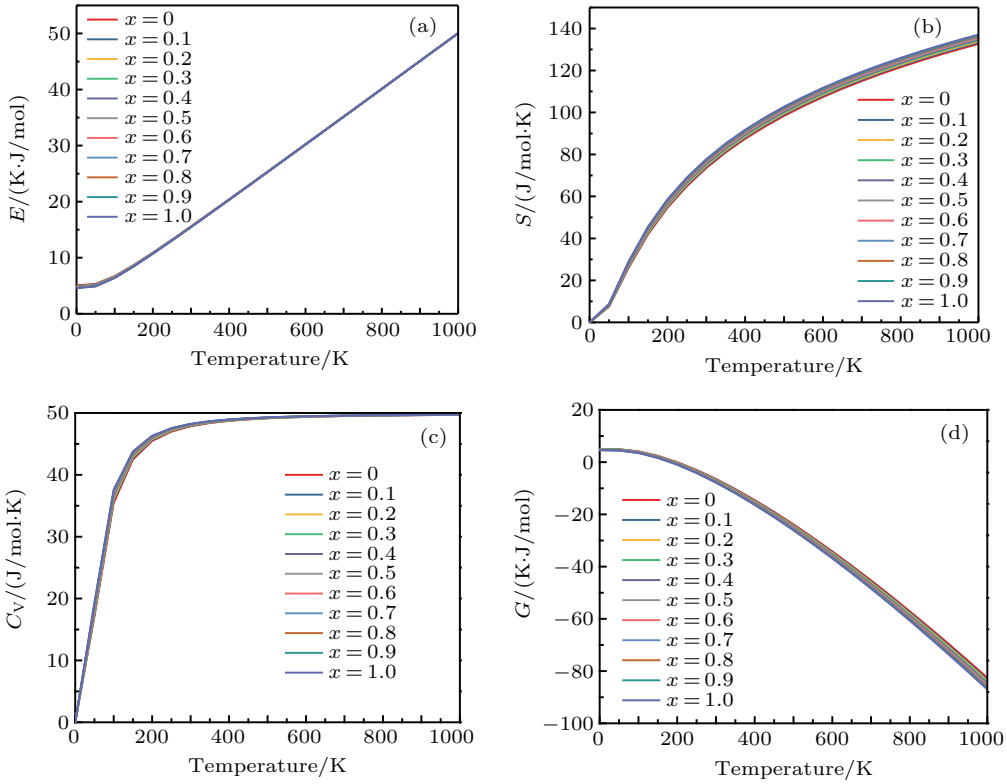


Fig. 6. (color online) Thermodynamic properties for $Zr_{1-x}Hf_xCo$: (a) internal energy E, (b) entropy S, (c) specific heat C_V, and (d) Gibbs free energy G.

Furthermore, in order to compare our calculated results with other reported theoretical results[16,19] and experimental[19] data for ZrCo, the calculated values of E, S, and C_V at selected temperatures ranging from 0 K to 1000 K for ZrCo are listed in Table 4. At a constant pressure, the change of enthalpy can be expressed as $\Delta H = \Delta E + P\Delta V$, where $P\Delta V$ is very small compared with ΔE in the solid phase, as a result in our work $\Delta H = \Delta E$. As can be seen from Table 4, our results are somewhat less than the experimental data reported by Chattaraj *et al.*, and the deviation increases with temperature increasing. The following reasons may cause the discrepancy: (i) in our calculation, the electronic contribution to the entropy S is neglected, and only the vibration entropy is considered;[43] (ii) our thermodynamic calculations are based on the harmonic approximation which has been successfully used to calculate the thermodynamic functions in most cases,[16,18,43–46] and the anharmonicity is ignored, whereas the effect of anharmonicity on thermodynamic function may be important and increased with temperature increasing;[43] (iii) the enthalpy increments in a temperature range from 642 K–1497 K are measured by using a high temperature inverse drop calorimeter and the following thermodynamic functions are derived from the measured enthalpy increments at 0.1 MPa,[19] but our calculations are based on an ideal single crystal under the 0 Pa. In comparison with the theoretical results, our calculated results of thermodynamic function are reasonably consistent with the results obtained from the PWSCF package and VASP code by Li *et al.*[16] and Chattaraj *et al.*[19] respectively. Accordingly, our predicted thermodynamic properties for $Zr_{1-x}Hf_xCo$ are reliable.

Table 4. Calculated and experimental data of E (K·J/mol), S (J/mol·K), $H - H_{298}$ (kJ/mol), C_V (kJ/mol) per unit cell of ZrCo.

T/K	E/(K · J/mol)		$H - H_{(298.15)}$(kJ/mol)		S/(J/mol.K)				C_V/(kJ/mol)		
	This work	Other cal.[a]	This work	Expt.[b]	This work	Other cal.		Expt.	This work	Other cal.	
						[a]Ref.	[b]Ref.	[b]Ref.		[a]Ref.	[b]Ref.
0	5.1				0		0		0		0
50	5.3				7.5		10.5		17.1		16.1
100	6.7				25.9		31.5		35.5		35.5
150	8.7				41.9		47.2		42.5		42.7
200	10.9				54.5		59.2		45.5		45.6
250	13.2				64.9		68.9		47.0		47.1
298.15	15.5		0	0	73.2		76.7	80.4	47.8		47.9
300	15.6	15.6	0.1	0.1	73.5	74.4		80.8	47.8	48.0	
400	20.4	20.4	4.9	5.3	87.4	88.4		95.6	48.7	48.9	
500	25.3	25.3	9.8	10.7	98.3	99.3		107.8	49.1	49.3	
600	30.2	30.3	14.7	16.4	107.3	108.3		118	49.4	49.5	
700	35.2	35.2	19.7	22.2	114.9	115.9		126.4	49.5	49.6	
800	40.1	40.2	24.6	28.1	121.6	122.6		135	49.6	49.7	
900	45.1	45.1	29.6	34.2	127.4	128.4		142.2	49.7	49.7	
1000	50.1	50.1	34.6	40.5	132.7	133.7		148.6	49.7	49.8	

[a]Ref. [16], [b]Ref. [19].

4. Conclusions

In summary, we investigate the structural, electronic, vibrational, and thermodynamic properties of $Zr_{1-x}Hf_xCo$ (x is the concentration of constituent element Hf, and changes from 0 to 1) using a first principles approach and the VCA method.

In our work, the equilibrium structures of $Zr_{1-x}Hf_xCo$ are investigated and reveal that as the Hf concentration x gradually increases from 0.0 to 1.0, the lattice constant reduces from 3.217 Å to 3.195 Å very slowly. In general, the obtained electronic structures of $Zr_{1-x}Hf_xCo$ exhibit similar behaviors, but further analysis indicates that the metallic nature is enhanced and the electrical conductivity turns better with the increase of Hf content. Moreover, as Hf concentration increases from 0 to 1, the Fermi energy gradually increases from −6.96 eV to −6.21 eV, and the $N(E_f)$ decreases from 2.795 electrons/eV f.u. to 2.594 electrons/eV f.u., both of which imply the decrease of chemical stability.

The dynamic properties with different Hf content in $Zr_{1-x}Hf_xCo$ compound are studied within DFPT, and the results show that the increase of Hf content makes the optical modes softened, the acoustical modes essentially unchanged, and the PHDOS significantly moves towards a low wave number generally. The maximum vibrational frequency decreases gradually from about 223 cm^{-1} to 186 cm^{-1}, which implies that there appear the lower scattering gradient and lower phonon group velocity with the decrease of the highest vibrational frequency. Finally, the complete thermodynamic data including internal energy E, constant-volume specific heat C_V, entropy S, and Gibbs free energy G are obtained and analyzed. The results demonstrate that there are small differences in the

thermodynamic property with the increase of the Hf content, and further analysis suggests that as the Hf content increases, the calculated values of the internal energy E and Gibbs free energy G decrease, while the entropy S and constant-volume specific heat C_V increase in the selected temperature ranges.

We expect some of our calculated results, such as thermodynamic quantities will provide useful information about tritium storage and transport.

Appendix A: Supplementary material

The data for parameters E, S, C, and G are listed in the following Tables S1–S4.

Table S1. The calculated result of internal energy E (K·J/mol) per unit cell for $Zr_{1-x}Hf_xCo$ at different temperature T (K), x represents the concentration of constituent element Hf.

T	x										
	0	0.1	0.2	0.3	0.4	0.5	0.6	0.7	0.8	0.9	1.0
0	5.063	4.979	4.908	4.847	4.796	4.751	4.708	4.670	4.634	4.604	4.573
100	6.720	6.659	6.609	6.566	6.531	6.502	6.475	6.452	6.431	6.413	6.396
200	10.904	10.868	10.839	10.814	10.794	10.778	10.762	10.749	10.737	10.729	10.718
300	15.593	15.568	15.568	15.548	15.531	15.517	15.506	15.495	15.486	15.478	15.472
400	20.427	20.417	20.408	20.393	20.380	20.370	20.361	20.353	20.346	20.340	20.335
500	25.322	25.323	25.307	25.295	25.284	25.276	25.269	25.263	25.257	25.252	25.248
600	30.248	30.259	30.236	30.225	30.217	30.209	30.204	30.198	30.194	30.190	30.186
700	35.192	35.211	35.181	35.172	35.165	35.159	35.154	35.149	35.145	35.142	35.139
800	40.147	40.173	40.137	40.130	40.123	40.118	40.113	40.109	40.106	40.103	40.100
900	45.109	45.142	45.101	45.094	45.088	45.083	45.080	45.076	45.073	45.070	45.068
1000	50.077	50.116	50.069	50.063	50.058	50.054	50.050	50.047	50.044	50.042	50.040

Table S2. The calculated result of entropy S (J/mol.K) per unit cell for $Zr_{1-x}Hf_xCo$ at different temperature T(K), x represents the concentration of constituent element Hf.

T	x										
	0	0.1	0.2	0.3	0.4	0.5	0.6	0.7	0.8	0.9	1.0
0	0	0	0	0	0	0	0	0	0	0	0
100	25.931	26.307	26.633	26.948	27.220	27.521	27.830	28.121	28.419	28.677	28.945
200	54.541	55.101	55.581	56.026	56.407	56.799	57.194	57.559	57.927	58.242	58.568
300	73.519	74.125	74.643	75.121	75.527	75.941	76.356	76.738	77.122	77.450	77.788
400	87.421	88.044	88.576	89.066	89.482	89.903	90.326	90.715	91.104	91.437	91.780
500	98.342	98.974	99.513	100.008	100.429	100.854	101.280	101.672	102.064	102.399	102.744
600	107.323	107.959	108.501	109.000	109.423	109.850	110.279	110.672	111.065	111.402	111.748
700	114.943	115.582	116.127	116.627	117.052	117.481	117.910	118.304	118.699	119.036	119.383
800	121.559	122.200	122.747	123.248	123.674	124.103	124.533	124.928	125.323	125.661	126.008
900	127.404	128.046	128.594	129.096	129.522	129.952	130.383	130.78	131.174	131.511	131.859
1000	132.638	133.281	133.829	134.332	134.759	135.189	135.620	136.016	136.412	136.750	137.098

Table S3. The calculated result of constant-volume specific heat C_V (J/mol·K) per unit cell for $Zr_{1-x}Hf_xCo$ at different temperature T (K), x represents the concentration of constituent element Hf.

T	x										
	0	0.1	0.2	0.3	0.4	0.5	0.6	0.7	0.8	0.9	1.0
0	0	0	0	0	0	0	0	0	0	0	0
100	35.479	35.852	36.168	36.441	36.671	36.869	37.057	37.222	37.378	37.507	37.638
200	45.481	45.639	45.770	45.879	45.969	46.044	46.114	46.173	46.228	46.273	46.317
300	47.845	47.923	47.988	48.041	48.085	48.121	48.154	48.183	48.209	48.230	48.251
400	48.721	48.767	48.804	48.835	48.861	48.882	48.901	48.917	48.932	48.945	48.957
500	49.136	49.165	49.190	49.210	49.226	49.240	49.252	49.263	49.273	49.281	49.289
600	49.363	49.384	49.401	49.415	49.427	49.436	49.445	49.452	49.459	49.465	49.470
700	49.501	49.517	49.529	49.540	49.548	49.555	49.562	49.567	49.572	49.576	49.580
800	49.591	49.603	49.613	49.621	49.627	49.633	49.638	49.642	49.646	49.649	49.652
900	49.653	49.662	49.670	49.676	49.682	49.686	49.690	49.693	49.696	49.699	49.701
1000	49.697	49.705	49.711	49.716	49.720	49.724	49.727	49.730	49.732	49.734	49.736

Table S4. The calculated result of Gibbs free energy G (K·J/mol) per unit cell for $Zr_{1-x}Hf_xCo$ at different temperature T (K), x represents the concentration of constituent element Hf.

T	x										
	0	0.1	0.2	0.3	0.4	0.5	0.6	0.7	0.8	0.9	1.0
0	5.063	4.979	4.908	4.847	4.796	4.751	4.708	4.670	4.634	4.604	4.573
100	4.127	4.029	3.945	3.871	3.809	3.750	3.692	3.640	3.589	3.546	3.501
200	–0.004	–0.152	–0.277	–0.391	–0.487	–0.582	–0.676	–0.762	–0.848	–0.921	–0.995
300	–6.463	–6.670	–6.845	–7.005	–7.141	–7.277	–7.412	–7.535	–7.658	–7.763	–7.871
400	–14.541	–14.809	–15.038	–15.246	–15.423	–15.600	–15.777	–15.940	–16.101	–16.240	–16.382
500	–23.849	–24.180	–24.462	–24.720	–24.938	–25.158	–25.377	–25.579	–25.780	–25.951	–26.128
600	–34.145	–34.540	–34.876	–35.183	–35.444	–35.706	–35.969	–36.209	–36.449	–36.654	–36.866
700	–45.268	–45.727	–46.117	–46.474	–46.778	–47.083	–47.388	–47.668	–47.947	–48.186	–48.432
800	–57.101	–57.623	–58.068	–58.475	–58.821	–59.169	–59.517	–59.837	–60.156	–60.428	–60.709
900	–69.554	–70.141	–70.640	–71.098	–71.487	–71.878	–72.269	–72.628	–72.986	–73.292	–73.608
1000	–82.561	–83.212	–83.766	–84.274	–84.705	–85.139	–85.574	–85.972	–86.370	–86.710	–87.060

References

[1] Devillers M, Sirch M, Bredendiek-Kämper S and Penzhorn R 1990 *Chem. Mater.* **2** 255

[2] Shmayda W, Heics A and Kherani N 1990 *J. Less-Common Met.* **162** 117

[3] Konishi S, Nagasaki T, Yokokawa N and Naruse Y 1989 *Fusion Eng. Des.* **10** 355

[4] Penzhorn R-D and Sirch M 1990 *J. Nucl. Mater.* **170** 217

[5] Qi Y, Ju X, Wan C B, Qiu J, Xub Y, Wang S M, Liu X P and Jiang L J 2010 *Int. J. Hydrogen Energy* **35** 2931

[6] Kou H Q, Huang Z Y, Luo W H, Sang S, Meng D Q, Luo D L, Zhang G H, Chen H, Zhou Y and Hu C W 2015 *Appl. Energy* **145** 27

[7] Jat R A, Parida S, Nuwad J, Agarwal R and Kulkarni S 2013 *J. Therm. Anal. Calorim.* **1** 37

[8] Hayashi T, Suzuki T, Konishi S, Yamanishi T, Nishi M and Kurita K 2002 *Fusion Sci. Technol.* **41** 801

[9] Shim M, Chung H, Cho S and Yoshida H 2008 *Fusion Sci. Technol.* **53** 830

[10] Konishi S, Nagasaki T and Okuno K 1995 *J. Nucl. Mater.* **223** 294

[11] Hara M, Okabe T, Mori K and Watanabe K 2000 *Fusion Eng. Des.* **49–50** 831

[12] Devillers M, Sirch M and Penzhorn R 1992 *Chem. Mater.* **4** 631

[13] Kou H Q, Sang G, Luo W H, Huang Z Y, Meng D Q, Zhang G H, Deng J, Luo Z P, He W B and Hu C W 2015 *Int. J. Hydrogen Energy* **40** 10923

[14] Zhao Y M, Li R F, Tang R H, Li B Y, Yu R H, Liu W, Koud H Q and Meng J B 2014 *J. Energy Chem.* **23** 9

[15] Peng L, Jiang C, Xu Q and Wu X 2013 *Fusion Eng. Des.* **88** 299

[16] Li G, Zhou H and Gao T 2012 *J. Nucl. Mater.* **424** 220

[17] Chattaraj D, Parida S, Dash S and Majumder C 2012 *Int. J. Hydrogen Energy* **37** 18952

[18] Chattaraj D, Parida S, Dash S and Majumder C 2015 *J. Alloys Compd.* **629** 297

[19] Chattaraj D, Jat R A, Parida S, Agarwal R and Dash S 2015 *Thermochim. Acta* **614** 16

[20] Lu W F, Li C J, Sarac B, Şopu C, Yi J H, Tan J, Stoica M and Eckert J 2017 *J. Alloys Compd.* **705** 445

[21] Gonze X, Beuken J M, Caracas R, Detraux F, Fuchs M, Rignanese G M, Sindic L, Verstraete M, Zerah G, Jollet F, Torrent M, Roy A, Mikami M, Ghosez P, Raty J Y and Allan D C 2002 *Comput. Mater. Sci.* **25** 478

[22] Perdew J P, Burke K and Ernzerhof M 1996 *Phys. Rev. Lett.* **77** 3865

[23] Nordheim L 1931 *Zur elektronentheorie der metalle. I. Annalen der Physik* **401** 607

[24] Yu C J and Emmerich H 2007 *J. Phys.: Condens. Matter* **19** 306203

[25] Bellaiche L and Vanderbilt D 2000 *Phys. Rev. B* **61** 7877

[26] Ghosez P, Desquesnes D, Gonze X and Rabe K 2000 *AIP Conf. Proc.* 102

[27] Bouamama K, Daoud K and Kassali K 2005 *Model. Simul. Mater. Sci. Eng.* **13** 1153

[28] Miao R, Huang G and Yang J 2016 *Solid State Commun.* **233** 30

[29] Bahloul B, Bentabet A, Amirouche L, Bouhadda Y, Bounab S and Deghfel B 2014 *J. Phys. Chem. Solids* **75** 307

[30] Bustamante-Romero I, De la Pe na-Seaman O, Heid R and Bohnen K P 2016 *J. Magn. Magn. Mater.* **420** 97

[31] Wei X P, Chu Y D and Deng J B 2014 *J. Magn. Magn. Mater.* **354** 345

[32] Yuan X L, Xue M A, Chen W and An T Q 2014 *Front. Phys.* **9** 219

[33] Konishi S, Nagasaki T, Hayashi T and Okuno K 1995 *J. Nucl. Mater.* **223** 300

[34] Flanagan T B, Noh H and Luo S 2016 *J. Alloys Compd.* **677** 163

[35] Gupta M 1999 *J. Alloys Compd.* **293–295** 190

[36] Yaar I, Gavra Z, Cohen D, Levitin Y, Kimmel G, Kahane S, Hemy A and Berant Z 1999 *Hyperfine Interact.* **120/121** 563

[37] Broyden C G 1970 *IMA. J. Appl. Math.* **6** 222

[38] Fletcher R 1970 *Comput. J.* **13** 317

[39] Goldfarb D 1970 *Math. Comput.* **24** 23

[40] Shanno D F 1970 *Math. Comput.* **24** 647

[41] Williamson I, Li S, Hernandez A C, Lawson M, Chen Y and Li L 2017 *Chem. Phys. Lett.* **674** 157

[42] Lee C and Gonze X 1995 *Phys. Rev. B* **51** 8610

[43] Ma S G, Shen Y H, Gao T and Chen P H 2015 *Int. J. Hydrogen Energy* **40** 3762

[44] Errea I, Rousseau B and Bergara A 2011 *Phys. Rev. Lett.* **106** 165501

[45] Norouzzadeh P, Myles C W and Vashaee D 2013 *J. Phys.: Condens. Matter* **25** 475502

[46] Liu B, Gu M and Liu X 2007 *Appl. Phys. Lett.* **91** 172102